Hose-Drum-Unit Modeling and Control for Probe-and-Drogue Autonomous Aerial Refueling

XUNHUA DAI
Beihang University, Beijing, China

ZI-BO WEI
Shanghai Aircraft Design and Research Institute, Shanghai, China

QUAN QUAN
KAI-YUAN CAI
Beihang University, Beijing, China

Probe-and-drogue aerial refueling has been widely adopted because of its flexibility, but the drogue is susceptible to wind disturbances, especially the receiver forebody bow wave disturbance and the excessive contact on the drogue. The docking process must be accurate, and a submeter error may result in failure. Thus, it is important for the docking task to understand the dynamics of the drogue under wind disturbances and improve safety after excessive contact happens. In this article, based on the previous work on drogue dynamic modeling, an improved integrated model is proposed by adding the hose-drum unit to describe the behavior of the drogue under wind disturbances more accurately. For the convenience of docking controller design of the receiver aircraft, the simplified drogue dynamic model with the hose-drum unit is obtained through system identification. Finally, to avoid the hose whipping phenomenon after excessive contact on the drogue, a control method is proposed to monitor the state of the hose and control the hose length to stabilize the drogue movement. Simulations and comparisons indicate that the motion of the drogue generated by the proposed modeling method is in good agreement with the real experimental results, and the proposed control method can significantly reduce the effect of the hose whipping phenomenon and improve the safety of probe-and-drogue aerial refueling systems.

Manuscript received October 23, 2017; revised August 12, 2018, April 13, 2019, and October 29, 2019; released for publication November 7, 2019. Date of publication November 14, 2019; date of current version August 7, 2020.

DOI. No. 10.1109/TAES.2019.2953413

Refereeing of this contribution was handled by Y. B. Shtessel.

This work was supported in part by the National Natural Science Foundation of China under Grant 61473012 and in part by the Beijing Municipal Natural Science Foundation under Grant L182037.

Authors' addresses: X. Dai, Q. Quan, and K.-Y. Cai are with the School of Automation Science and Electrical Engineering, Beihang University, Beijing 100191, China, E-mail: (dai@buaa.edu.cn; qq_buaa@buaa.edu.cn; kycai@buaa.edu.cn). Z.-B. Wei was with the School of Automation Science and Electrical Engineering, Beihang University, Beijing 100191, China; He is now with the Shanghai Aircraft Design and Research Institute, Shanghai 200120, China, Email: (weizibo@comac.cc). *(Corresponding authors: Xunhua Dai; Quan Quan.)*

I. INTRODUCTION

Autonomous aerial refueling (AAR) increases the endurance and range of unmanned aerial vehicles [1]–[3] by refueling them in flight [4]. Probe-and-drogue refueling (PDR) is widely adopted in AAR because of the simplicity of the equipment and its flexibility. In a PDR system, there is a hose payout and reel-in device, which is called a hose-drum unit (HDU) [5] (also known as the reel take-up system [6], [7]). It consists of a hose-drum motor and a motor control unit and determines the motion of the upper end of the hose [5]. It is an important device for suppressing the hose whipping phenomenon (HWP), which can result in severe damage to the probe or the drogue [8].

HWP is caused by excessive contact between the probe and the drogue. The existing literature, such as [6] and [8], focuses on how to design an HDU controller so as to maintain the tension of the hose and suppress HWP. In practice, the drogue will remain relatively static if the hose–drogue system is not affected by wind disturbances. In this situation, "excessive contact" is hard to happen because tracking a static target is a relatively easy and simple task. However, due to wind disturbances, the drogue always moves, so the receiver has to speed up to chase the drogue, which may result in excessive contact and the HWP. In addition to suppressing the HWP after the contact, this article tries to reveal that the HDU can also be applied as a feed back damper to reduce the frequency and amplitude of the drogue position fluctuation under wind disturbances, which did not attract enough attention in previous research. Fortunately, basic models were established by the existing literature, which can be employed to analyze the dynamics of the drogue with the HDU controller. The hose–drogue dynamic model is established, and the behavior of the drogue in the docking stage is analyzed in [5]–[7], [9], and [10].

In the whole refueling process, the motion of the drogue is influenced by many types of wind disturbances, such as the aerodynamic effect of the tanker [11], atmospheric turbulence [12], the bow wave effect [13], and so on. According to the NASA flight test results [13], as shown in Fig. 1(a), the drogue fluctuates with the amplitude of about 0.1–0.2 m (mainly caused by atmospheric turbulence; the amplitude depends on the weather condition) in a low frequency when the receiver is far away. When the receiver comes close to the drogue, the drogue is quickly pushed away by the bow wave flow field with an offset of about 0.4 m [see the dotted ellipse region in Fig. 1(a)], and this docking attempt fails because the probe is too slow to chase the drogue. As a result, in the docking stage, the bow wave of the receiver is the most substantial one. Thus, the hose–drogue model under the bow wave is simplified in [14] and [15], which is called the drogue dynamic model. Moreover, the motion of the drogue under the bow wave and its control

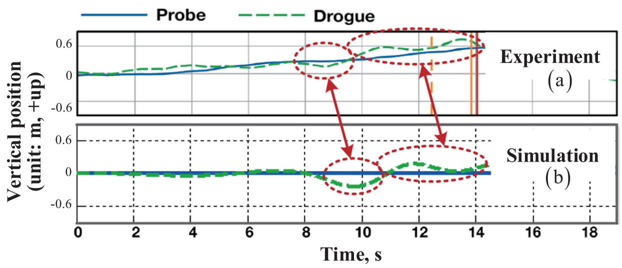

Fig. 1. Vertical motion of the drogue in [14]. (a) Experiment. (b) Simulation.

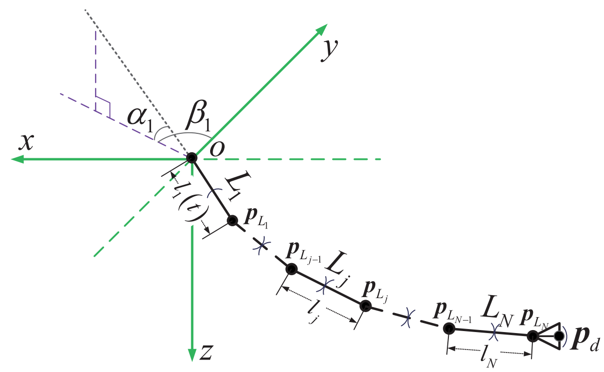

Fig. 2. Flexible hose–drogue dynamic model expressed by a series of rigid links.

methods are studied in [16]–[18]. However, there are some differences (the dotted ellipse regions in Fig. 1) between the simulation results generated by the drogue dynamic model [see Fig. 1(b)] and the results generated by the flight test experiment [see Fig. 1(a)] [13]; the simulation results are about 40% larger than the experimental results, especially for the vertical position. One of the main reasons is that the effects of the HDU were not considered by the drogue dynamic model. Thus, the results of [14] have been improved in this article by considering the effects of the HDU. Meanwhile, the traditional HDU control methods mainly feed back the hose tension to reduce the drogue fluctuation and suppress the HWP to some extent, but it cannot avoid the HWP essentially because it cannot detect the occurrence of the HWP and its degree. Since the HWP is essentially caused by the overslack of the hose due to excessive contact on the drogue, this article proposes an anti-HWP control method to monitor the state of the hose and control the hose length to stabilize the drogue movement.

In summary, the main contributions of this article are as follows.

1) A more precise modeling method for the hose-and-drogue system is proposed based on the previous study.
2) By considering the effects of the HDU controller, an improved integrated model is proposed to describe the behavior of the drogue under wind disturbances more accurately, and a simplified drogue dynamic model is obtained through system identification for the convenience of docking controller design of the receiver aircraft.
3) Improvements are proposed for traditional HDU controllers for realizing a better performance to stabilize the drogue position under disturbances before the contact happens.
4) For excessive contact situations, an anti-HWP control method is proposed to significantly reduce the effect of the HWP and improve the safety of aerial refueling systems.

The rest of this article is organized as follows. Section II reviews the drogue dynamic model without the HDU controller and analyzes its limitations. Section III describes the models used in the simulation and demonstrates the procedure of researching the effects of the HDU. Section IV compares two types of controllers for the HDU, and the corresponding drogue dynamic models with HDU controllers are obtained by following the procedure of the simulation, as mentioned in Section III; their performances are also compared in this section. The anti-HWP control method is proposed and verified in Section V. Finally, Section VI concludes this article.

II. DYNAMICS OF THE DROGUE WITHOUT THE HDU CONTROLLER

A drogue dynamic model without an HDU is proposed in [14]. In order to make this article self-contained, this model is introduced briefly in this section. Then, the problem of this model is analyzed in the rest of this section.

A. Drogue Dynamic Model Without the HDU Controller

A flexible hose–drogue dynamic model is often expressed by a series of rigid links according to the finite-element method, which is called the link-connected model [19]. As shown in Fig. 2, the orientation of each link L_j with the length l_j is described by its orientation angles $\alpha_j \in \mathbb{R}$, $\beta_j \in \mathbb{R}$, $j = 1, 2, \ldots, N$, where $N \in \mathbb{Z}^+$ is the number of rigid links. If a hose–drogue dynamic model with a fixed-length hose (fixed-length hose–drogue model for short) is considered, then each lumped mass position $\boldsymbol{p}_{L_j} \in \mathbb{R}^3$ and velocity $\dot{\boldsymbol{p}}_{L_j} \in \mathbb{R}^3$ are expressed by $\alpha_j, \beta_j, \dot{\alpha}_j, \dot{\beta}_j$, and l_j. Moreover, for a hose–drogue dynamic model with a variable-length hose (variable-length hose–drogue model for short), $\boldsymbol{p}_{L_j}$ and $\dot{\boldsymbol{p}}_{L_j}$ are expressed by $\alpha_j, \beta_j, \dot{\alpha}_j, \dot{\beta}_j, l_j$, and $\dot{l}_j$.

All of these variables are measured in the tanker frame $(o - xyz)$. The origin of this frame o is set to the conjunctive point between the tanker and the hose, and the frame axes (x, y, z) are aligned with the wind frame forward-right-down directions of the tanker; namely, the direction of ox is identical with the velocity of the tanker. Under this frame, a fixed-length hose–drogue model without the HDU controller is established in [14]. Then, it is linearized when $h = 3000$ m and $v_T = 120$ m/s.

The simplified system is the drogue dynamic model for the drogue offset position $\Delta \boldsymbol{p}_d \triangleq \boldsymbol{p}_d - \boldsymbol{p}_d(0)$, where $\boldsymbol{p}_d = [p_{dx}, p_{dy}, p_{dz}]^{\mathrm{T}} \in \mathbb{R}^3$ is the position of the drogue. The transfer function for the drogue dynamic is as shown

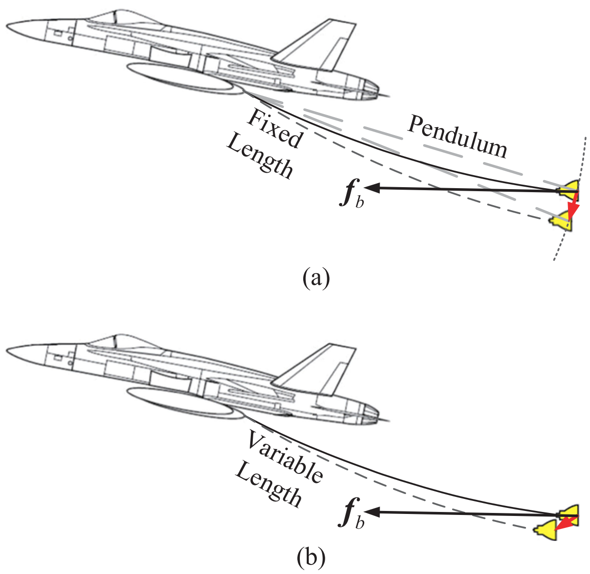

Fig. 3. Motion of the drogue (a) without and (b) with the HDU controller.

in the following equation [14]:

$$\Delta \boldsymbol{p}_d(s) = \begin{bmatrix} G_{xx}(s) & 0 & G_{zx}(s) \\ 0 & G_{yy}(s) & 0 \\ G_{zx}(s) & 0 & G_{zz}(s) \end{bmatrix} \boldsymbol{f}_b(s) \qquad (1)$$

where $\boldsymbol{f}_b = [f_{bx}, f_{by}, f_{bz}]^{\mathrm{T}} \in \mathbb{R}^3$ is the disturbance force input acting on the drogue. Moreover, under a fixed flight condition (the height h and the airspeed v_T of the refueling), if the hose–drogue device is not influenced by any disturbance, the drogue will reach a steady position, which is noted by $\boldsymbol{p}_d(0)$. The detailed expressions for (1) can be found in our previous work [14].

B. Limitations of the Drogue Dynamic Model Without the HDU Controller

According to [14], vertical motions of the drogue in the simulation and the experiment are somewhat different, as shown in Fig. 1. An important reason causing this phenomenon is that the gains of G_{zx} and G_{zz} are much larger than that of G_{xx} and G_{zx}, respectively. It means that both f_{bx} and f_{bz} influence p_{dz} much more than p_{dx}. This phenomenon can be explained by an intuitive example as follows. When the drogue reaches the steady position, the hose is tight. The hose–drogue device is similar to a pendulum in this situation [20], as shown in Fig. 3(a). Thus, with a small range, the motion of the drogue is close to a circular arc around the upper end of the hose, no matter on which direction the force acts on it. Because the length of the hose cannot be changed, the vertical motion and the longitudinal motion of the drogue are coupled tightly, and the corresponding drogue dynamic model cannot accurately describe the behavior of the drogue in practice. On the other hand, the HDU modifies the dynamics of the drogue by changing the length of the hose, as shown in Fig. 3(b). Thus, it is important to research the effects of the HDU acting on the dynamics of the drogue.

III. HOSE–DROGUE MODEL WITH THE HDU CONTROLLER UNDER THE BOW WAVE EFFECT

According to the previous section, the fixed-length hose–drogue model under the bow wave has been analyzed in [14]. However, this model needs to be replaced by a variable-length hose–drogue model and an HDU model to obtain the dynamics of the drogue more accurately. Thus, the bow wave model and these two models are introduced first. Then, the procedure of the simulation is illustrated.

A. Three Models Used in the Simulation

1) *Bow Wave Model:* The bow wave is a complex disturbance caused by the receiver forebody flow field. Based on modeling and simulation methods [5]–[7], [21] of the hose–drogue dynamics, Bhandari *et al.* [22] established the bow wave effect model as a lookup table, and then, Wei *et al.* [14], [15] modeled it as explicit equations. In order to compare the results of this article with those of [14], the bow wave model in [14] is employed.

2) *Variable-Length Hose–Drogue Model:* The variable-length hose–drogue model is also based on the link-connected model. There are two kinds of variable-length hose–drogue model: 1) only the length of the first link l_1 is variable [5] and 2) the variation of the hose is assigned equally to every link [8]. Since the variation of the hose is not remarkable before the impact happens, the former model is adopted for simulations without considering the intense contact on the drogue to reduce the computational cost. Refer to [5] for details.

3) *HDU Model:* The HDU system for hose payout and reel-in is modeled as a drum (or reel) [5], [6]. The dynamical motion of the drum can be described as

$$(T_{\mathrm{reel}} - T_{\mathrm{hose}})\, r_{\mathrm{reel}} = I_{\mathrm{reel}} \alpha_{\mathrm{reel}} \qquad (2)$$

where r_{reel} is the drum radius of the reel system, I_{reel} is the moment of inertia of the drum, and α_{reel} is the angular acceleration. The tension of L_1 is T_{hose} because the tension of the whole hose acts on it, and T_{reel} is the tension of the reel. Let l denote the total length of the hose, i.e.,

$$l = \sum_{i=1}^{N} l_i \qquad (3)$$

where N is the number of the links and l_i is the length of the ith link. If the reel is modeled as a thin circular cylindrical shell, then $I_{\mathrm{reel}} = m_{\mathrm{reel}} r_{\mathrm{reel}}^2$, where m_{reel} is the weight of the reel. On the other hand, the angular acceleration α_{reel} can be expressed regarding the linear acceleration, which means $\alpha_{\mathrm{reel}} = \ddot{l}/r_{\mathrm{reel}}$. Thus, (2) becomes

$$\ddot{l} = \frac{T_{\mathrm{reel}} - T_{\mathrm{hose}}}{m_{\mathrm{reel}}}. \qquad (4)$$

Note that, if only the first link has a variable length, then there are $\ddot{l} = \ddot{l}_1$ and $\dot{l} = \dot{l}_1$; if all the links have a variable length, then $\ddot{l}/N = \ddot{l}_i$ and $\dot{l}/N = \dot{l}_i$.

The relation among the bow wave model, the variable-length hose–drogue model, and the HDU model is shown

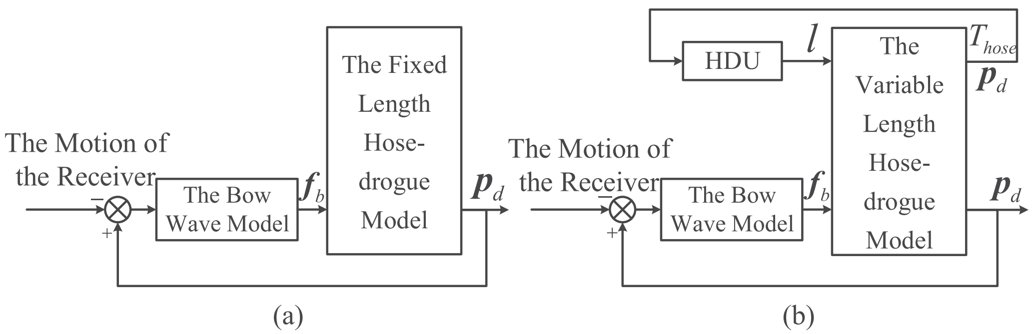

Fig. 4. Relation between the models (a) without and (b) with the HDU controller.

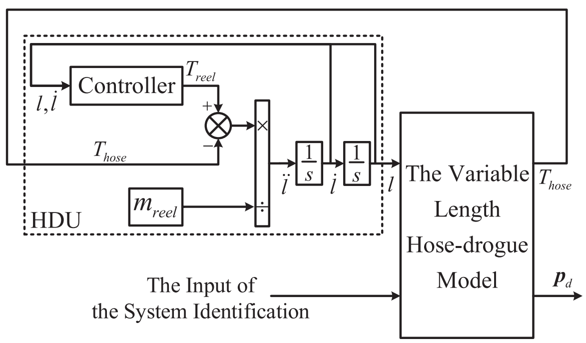

Fig. 5. *Simulation 1*: The simulation used in system identification.

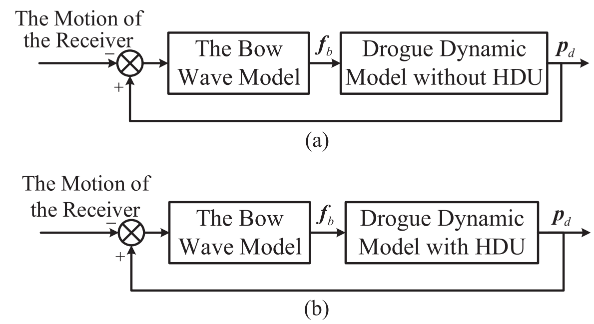

Fig. 6. *Simulation 2*: The simulation used in the final comparison. (a) Motion of the drogue generated by the drogue dynamic model without the HDU controller. (b) Motion of the drogue generated by the drogue dynamic model with the HDU controller.

in Fig. 4(b), while the relation of the models used in [22] is shown in Fig. 4(a).

B. Procedure for Researching the Effects of the HDU

The controller in the HDU can adjust the tension T_{reel} in (4) and, consequently, influences the dynamics of the drogue through changing the length of the hose. How the controller influences the dynamics of the drogue is the main issue in the rest of this article. This issue is analyzed by two simulations: Simulation 1 is used in system identification, and Simulation 2 is used to compare the effects of the drogue dynamic models with and without the HDU controller. These simulations are organized by the following procedure, and the procedure is realized in the next section.

First, Simulation 1 is established, which contains the variable-length hose–drogue model and the HDU model. The structure of the simulation is illustrated in Fig. 5, which is the same as the models between $\boldsymbol{f}_b$ and $\boldsymbol{p}_d$ in Fig. 4(b).

Second, two types of controllers are set into the "Controller" block, and step signals are employed to stimulate the system in Simulation 1. The response data of the system are used to analyze the effects of different controllers with different parameters' preliminary.

Third, based on Simulation 1, the system identification method is employed to obtain the linearized models, which are the drogue dynamic models with the HDU controller. These models can express the dynamics of the drogue with HDU controllers, which are controlled by different controllers. The input of the system identification method is the force acting on the drogue, which is equivalent to the bow wave force $\boldsymbol{f}_b$, and the output is the position of the drogue $\boldsymbol{p}_d$. The procedure of the system identification method is the same as that in [14]. Through the linearized models, different effects caused by different controllers are further analyzed.

Finally, Simulation 2 is established. The structure of this simulation is the same as that of the final simulation of [14], as shown in Fig. 6(a). However, in this article, the drogue dynamic model without the HDU controller is replaced by the drogue dynamic models with HDU controllers, as shown in Fig. 6(b). The simulation results of Simulation 2 are the motions of the drogue generated by the drogue dynamic model with and without the HDU controller. They are compared in the next section. It should be noted that, unlike the complex nonlinear models used in Fig. 4, the models of Fig. 6 are simple linearized models.

IV. CONTROLLERS OF THE HDU AND THE CORRESPONDING DROGUE DYNAMIC MODELS

In this section, two types of controllers are designed for the HDU, and the corresponding drogue dynamic models with HDU controllers are obtained. This section is introduced by following the procedure introduced in Section III-B.

A. Parameters of the Simulations

The parameters of Simulations 1 and 2 are the same as those in [14]. However, the new parameters used in the

TABLE I
Parameters of the Simulations

Parameter	Value	Unit
Number of the links, N	10	
Full length of the hose, L_h	15	m
Initial length of L_1, $l_1(0)$	2	m
Length of other links, $L_j, j = 2, 3, \ldots, N$	13/9	m
Weight of the reel, m_{reel}	68	kg
Initial tension of the hose, $T_{hose}(0)$	1610	N

HDU model and the variable-length hose–drogue model are listed in Table I. Here, the length of the first link is variable, and the length of the rest hose is divided into the other links, which are constant. The initial tension of the hose T_0 means the hose tension without disturbance when the whole hose is released. Then, Simulations 1 and 2 are established according to Figs. 5 and 6.

B. Two Types of Controllers

Simulation 1 is employed in this section, and two types of controllers are considered. First, one type of controller for the HDU is proposed in [5] and [6] as

$$T_{\text{reel}}(t) = T_{\text{hose}}(0) \cdot \left[\frac{l_1(t)}{l_1(0)}\right]^k, \quad 0 < l_1(t) \leq l_1(0). \qquad (5)$$

Under this controller, the HDU responds by reeling in the hose as the drogue is influenced by disturbances. The parameter of the controller is set as $k = \{0.3, 0.5, 1, 3\}$, and the simulation results are shown in Fig. 7(a1)–(a4), which illustrates the responses of $T_{\text{hose}}(t)$, $l_1(t)$, and $\boldsymbol{p}_d(t)$, respectively. For the convenience of observing the dynamic response of the HDU controller, a step disturbance force $\boldsymbol{f}_b$ [from (0, 0, 0) to (75, 0, 0)] is injected into the hose–drogue system at $t = 100$. In order to simulate the disturbance intensity in a real condition, the amplitude of the step disturbance is selected according to the average amplitude of the bow wave effect obtained by computational fluid dynamics (CFD) methods. The reason of using this input is that at the beginning part of the docking stage, only $f_{bx} > 0$, while $f_{by} = f_{bz} = 0$. Moreover, in this part, the differences (as shown in Fig. 1) between [14] and the experiment in [13] begin to emerge, and a 40% modeling error is observed in the vertical position.

According to Fig. 7(a1)–(a4), the transient processes of the responses oscillate initially, although the tension recovers its balance again at last. Thus, in order to improve the transient processes, the damping is introduced to the controller, and the new type of controller is

$$T_{\text{reel}}(t) = T_{\text{hose}}(0) \cdot \left[\frac{l_1(t)}{l_1(0)}\right]^k + k_d \dot{l}_1(t) \qquad (6)$$

where $0 < l_1(t) \leq l_1(0)$ and $k_d \in \mathbb{R}_+$. The variable $\dot{l}_1(t)$ can be measured directly or through the rotational speed of the reel indirectly, so the controller is realizable. By employing controller (6), the simulation results are shown in Fig. 7(b1)–(b4), when $k_d = 500$. It is obvious that the transient processes are much better than before.

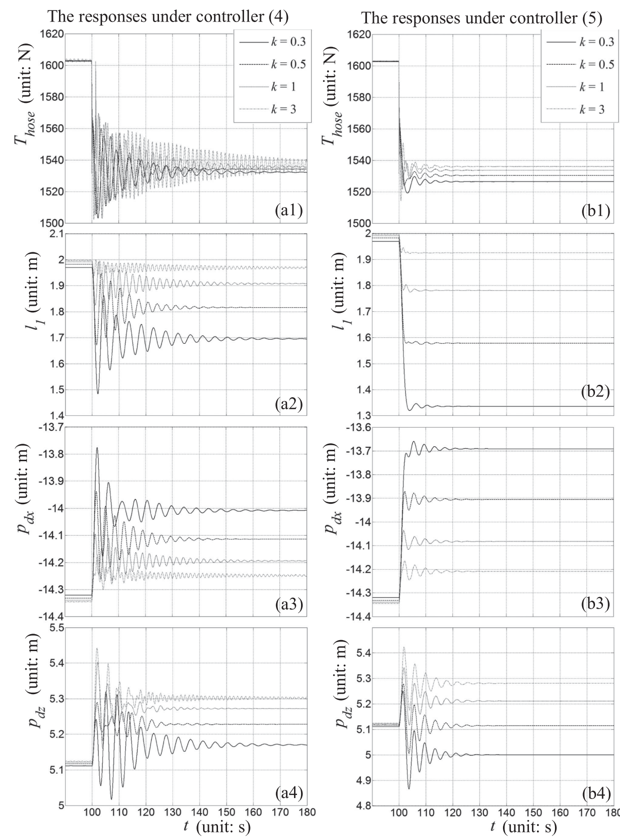

Fig. 7. Responses under the two types of controllers (the output p_{dy} is omitted because its response is always 0 in this situation). (a1)–(a4) Responses under controller (4). (b1)–(b4) Responses under controller (5).

Moreover, according to Fig. 7, the effects of the parameter k are summarized as follows.

1) The final tension is not influenced by k remarkably, as shown in Fig. 7(a1) and (b1).
2) The length that is reeled in by the HDU is influenced by k remarkably, as shown in Fig. 7(a2) and (b2). If k is small, the HDU needs to reel in the longer hose to achieve the same final tension. Otherwise, if the hose length needs to be changed as small as possible, then a large k can be chosen.
3) A larger k will bring negative effects, which will make the system tend to be unstable, according to Fig. 7(a1) and (a2). Actually, for controller (5) and $k = 4$, the outputs are divergent. Controller (6) can improve this situation significantly.
4) The parameter k influences the dynamics of the drogue indirectly through the variation of the hose length, according to Fig. 7(a3), (a4), (b3), and (b4). This property will be analyzed further in the next subsection.

C. Drogue Dynamic Model With Different HDU Controllers

Based on Simulation 1, the system identification is employed to obtain the linearized models, which are known as the drogue dynamic model with the HDU controller. The procedure of the system identification method is the

TABLE II
Drogue Dynamic Model With Two HDU Controllers as $k=0.5$

		Transfer Function	Fitness
Controller (4)	G_{xx}	$\frac{0.012s^2+0.012s+0.052}{s^4+2.15s^3+9.17s^2+7.54s+18.21}$	84.9%
	G_{xz}	$\frac{0.0010s^2+0.0057s+0.046}{s^4+13.49s^3+19.29s^2+35.69s+29.50}$	70.9%
	G_{yy}	$\frac{0.026s^2+0.0034s+0.42}{s^4+0.39s^3+24.02s^2+5.76s+49.66}$	99.5%
	G_{zx}	$\frac{0.0026s^2+0.010s+0.032}{s^4+1.76s^3+11.03s^2+7.04s+20.01}$	85.1%
	G_{zz}	$\frac{0.027s^2+0.0011s+0.38}{s^4+0.56s^3+24.22s^2+7.063s+53.95}$	94.5%
Controller (5)	G_{xx}	$\frac{0.0090s^2+0.011s+0.021}{s^4+4.01s^3+6.61s^2+10.48s+7.382}$	98.3%
	G_{xz}	$\frac{0.0048s^2+0.019s+0.0085}{s^4+3.29s^3+5.77s^2+8.44s+5.80}$	98.5%
	G_{yy}	$\frac{0.026s^2+0.0033s+0.42}{s^4+0.40s^3+24.01s^2+5.75s+49.62}$	99.6%
	G_{xz}	$\frac{0.0051s^2+0.0091s+0.0051}{s^4+1.96s^3+4.32s^2+4.71s+3.14}$	93.2%
	G_{zz}	$\frac{0.027s^2+0.0046s+0.39}{s^4+0.61s^3+24.05s^2+7.71s+55.76}$	96.3%

TABLE III
DC Gains of the Drogue Dynamic Model With Different HDU Controllers and Without HDU Controller

	With HDU Controller					No HDU Control
	Contr.	$k=0.3$	$k=0.5$	$k=1$	$k=3$	
G_{xx}	(5)	41.60	28.69	18.96	12.59	8.15
	(6)	42.04	28.98	19.15	12.64	
G_{zx}	(5)	8.08	14.48	20.07	23.56	22.94
	(6)	7.42	14.56	19.93	23.52	
G_{yy}	(5)	84.65	84.58	84.72	84.75	82.29
	(6)	84.65	84.68	84.73	84.75	
G_{xz}	(5)	11.81	15.98	19.78	21.77	8.15
	(6)	11.48	16.31	19.54	21.78	
G_{zz}	(5)	72.42	69.99	68.22	67.13	66.32
	(6)	72.02	69.76	68.20	67.08	

The magnitude of the values in the table is 10^{-4}.

same as that in [14]. System Identification Toolbox [23] of MATLAB is employed to identify the system, and the simulation used in the identification is as shown in Fig. 5. Then, the two identified systems are shown in Table II, which demonstrate the dynamics of the drogue under controller (5) and controller (6) with $k = 0.5$. The quantitative quality assessment of estimation is shown by Fitness F in Table II, which is calculated by $F = 1 - \|\boldsymbol{y} - \hat{\boldsymbol{y}}\|/\|\boldsymbol{y} - \bar{\boldsymbol{y}}\|$, where $\boldsymbol{y}, \hat{\boldsymbol{y}},$ and $\bar{\boldsymbol{y}}$ are the real output, the estimation of the output, and the mean of the real output, respectively.

Unlike the drogue dynamic model without the HDU controller, fourth-order transfer functions are employed to identify the drogue dynamic model with the HDU controller. The reason is that besides the second-order dynamics of the drogue without the HDU controller, additional second-order transfer functions are needed to describe the dynamics of the HDU, according to (4). Thus, the fourth-order identification results are much better than the second-order ones, and the fourth-order transfer functions are adopted. Then, according to Table II, the following conclusions about the dynamics of the drogue are obtained.

1) The transient process of the dynamics of the drogue under controller (6) is much better than that under controller (5). The reason is that controller (6) makes the poles far away from the imaginary axis.
2) According to Fitness in Table II, the effect of identification for controller (5) is worse than that under controller (6). The reason is that the behavior of the drogue under controller (6) is closer to outputs of linear systems than that of under controller (5), as shown in Fig. 7(a3) and (a4). Thus, if a linear model is used to express the dynamics of the drogue with the HDU controller, the system under controller (6) is more appropriate.
3) By comparing the gains of the transfer functions in Table II and that of (1), it is obvious that the dynamics of the drogue is very different when the system is with or without the HDU controller. In order to demonstrate the differences in detail and analyze the influences of different k, the dc gains [24, p. 94] under the two controllers with $k = \{0.3, 0.5, 1, 3\}$ are shown in Table III.

According to Table III, the following conclusions about the dynamics of the drogue are obtained.

1) The gains of the transfer functions under controllers (5) and (6) are similar, which means that the controller (6) does not change the final value of the system.
2) When k is small, the effects acting on the gains, which are caused by HDU, are remarkable, especially for $G_{xx}(s)$ and $G_{zx}(s)$. The x channel and the z channel are decoupled perfectly, which means the gains of $G_{zx}(s)$ and $G_{xz}(s)$ are much smaller than that of $G_{xx}(s)$ and $G_{zz}(s)$, respectively. Conversely, when k is large, the x channel and the z channel are coupled seriously. When k is large enough, such as $k = 3$, the gains with the HDU controller approach the gains without the HDU controller.
3) The effects acting on the gains of the y channel by the HDU are not remarkable.

Above all, if the purpose of the HDU is to suppress the HWP, then k should be chosen as a large number. On the other hand, if the purpose of the HDU is to decouple the dynamics of the drogue, then k should be chosen as a small number. Thus, k should be chosen to balance these two properties. Moreover, regardless of the value of k, it is necessary to choose controller (6) for the HDU to obtain a better transient process.

REMARK 1 The results in Table II are obtained without crosswind. If the crosswind in the refueling environment is remarkable, the y channel will be coupled with x and z channels. That means G_{yx}, G_{xy}, G_{zy}, and G_{zy} will not be zero. However, they can also be identified. Moreover, in

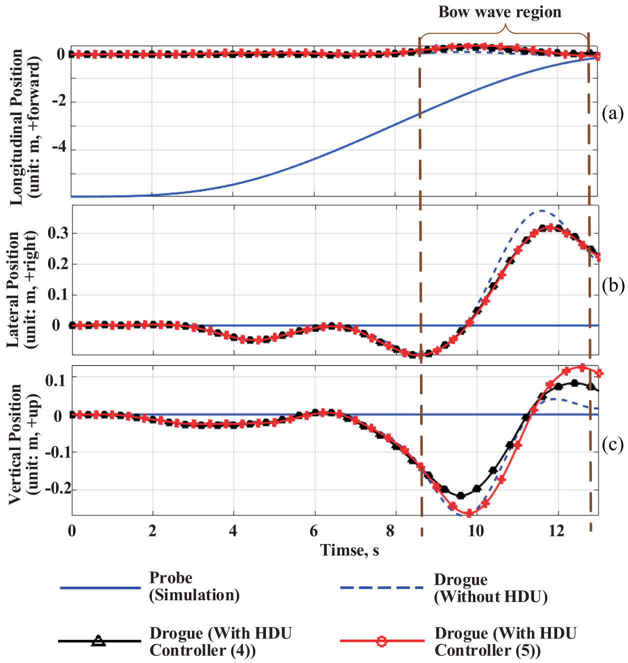

Fig. 8. (a)–(c) Comparison of motions of the drogue under the following situation: 1) the simulation results without the HDU controller; 2) the simulation results with the HDU controller (5) as $k = 0.5$; and 3) the simulation results with the HDU controller (6) as $k = 0.5$.

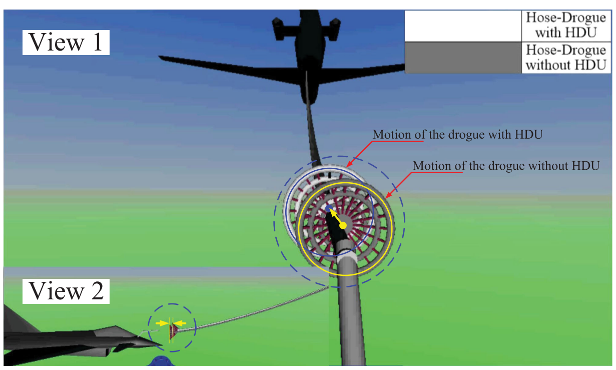

Fig. 9. Screenshot of the video. (View 1 is from the pilot view, and View 2 is from the side view.)

general situations, the crosswind is not remarkable, and the y channel is decoupled with x and z channels according to [14].

D. Comparison of Dynamics of Drogue With and Without the HDU Controller

According to Simulation 2, in order to demonstrate the effect acting on the dynamics of the drogue by the HDU, the corresponding parts of models used in [14] are replaced by the drogue dynamic models with HDU controllers, which are shown in Table II. The motions of the drogue under different situations are illustrated in Fig. 8. The corresponding video is available online[1] and the screenshot is shown in Fig. 9.

[1][Online]. Available: https://youtu.be/zcm6D1Gfcbg

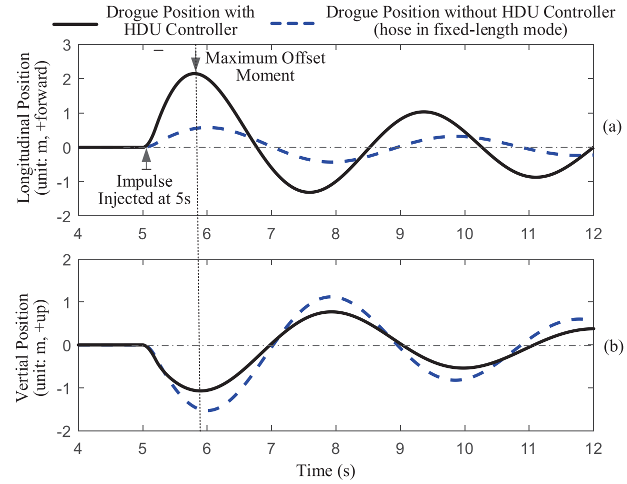

Fig. 10. (a) and (b) Comparison of motions of the drogue after excessive contact.

According to Fig. 8, the HDU influences the dynamics of the drogue slightly. However, the docking process must be an accurate task, and a submeter error may result in failure. Thus, the slight influence is important. Fig. 8(b) and (c) shows the detailed changes in the vertical position. Moreover, as shown in the bow wave region of Fig. 9, the drop in the vertical position is decreased, and the length of the hose is adjusted by the HDU remarkably. Compared with our previous results in [14], the motion of the drogue with the HDU controller (5) is closer to the motion in the experiment than the motion without the HDU controller. That means the drogue dynamic model under controller (5), which is a commonly used controller, approximates to the actual situation. On the other hand, because the HDU under controller (6), which is a new controller, adjusts the hose faster than controller (5), the dynamics of the drogue are different from those under the commonly used controller. However, controller (6) is supposed to be adopted in the future HDU controller design, because its smooth transient process is helpful for suppressing HWP and linearizing the hose–drogue model.

E. Effect of HWP Suppression of Traditional HDU Control Methods

In order to estimate the effect that the traditional HDU control methods suppress the HWP after excessive contact between the probe and the drogue, comparison simulations are performed, and the results are shown in Fig. 10, where an impulse disturbance (500 N· s) is injected into the hose–drogue system at 5 s to simulate excessive contact on the drogue. It can be observed from Fig. 10 that the hose–drogue system with the HDU controller has a larger longitudinal offset and a smaller vertical offset than that of the hose–drogue system without the HDU controller, where the larger longitudinal offset is caused by the hose being reeled up by the HDU controller to avoid a vertical offset. The vertical offset indicates that the current HDU control methods can suppress the HWP to some extent, but the effect is very limited, and it cannot avoid the HWP essentially. In the

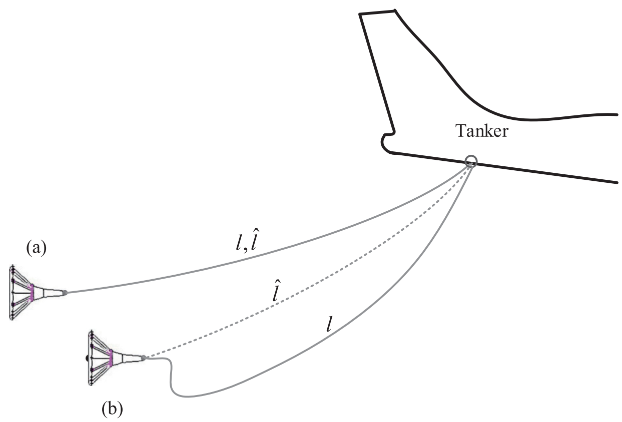

Fig. 11. Schematic diagram for the HWP. The symbol l is the hose length and $\hat{l}$ is the desired hose length. (a) Normal situation. (b) Hose overslack situation.

next section, a new HDU controller is proposed to avoid the HWP and improve the safety of probe-and-drogue systems.

V. ANTI-HWP CONTROL METHOD FOR THE HDU

The traditional HDU control methods mainly feed back the hose tension to reduce the drogue fluctuation and suppress the HWP to some extent, but it cannot avoid the HWP essentially because it cannot detect whether the HWP happens. For example, when the probe is docked into the drogue, it may drive the drogue to continue to move forward a distance, which may cause the hose slack and reach to a new equilibrium state, as shown in Fig. 11(b). In this situation, the hose tension remains unchanged so the traditional HDU control methods cannot work correctly, but the HWP will happen if the probe accidentally breaks away from the drogue. Therefore, the HWP is essentially caused by the overslack of the hose due to excessive contact on the drogue. In order to avoid the HWP, the HDU controller must be able to observe the hose slack degree and roll up the hose with an appropriate control method. This section will present an anti-HWP control method from three aspects: HWP observation, control method, and simulation verification.

A. HWP Observation

1) *Drogue Position Estimation:* The most direct way to detect the HWP is to observe the shape of the hose through computer vision methods, but it is impractical and unreliable for real aerial refueling systems. Observing the position of the drogue $\boldsymbol{p}_d$ to estimate the hose slack degree indirectly for the HWP is a more feasible way, which is adopted in this article. The drogue position $\boldsymbol{p}_d$ is essential for the docking control of the AAR system to estimate the relative position between the probe and the drogue. There are many mature methods to estimate the drogue position, among which the vision-based methods [13], [25] are the most convenient and widely used one. These methods can be applied to estimate the drogue position for the following HDU control method.

2) *Hose Slack Degree:* With the drogue position $\boldsymbol{p}_d$ and the total hose length l, how to define the hose slack degree and how to estimate it are presented in this subsection. First of all, the normal situation with no hose slack is presented, as shown in Fig. 11(a), which is the equilibrium state of the hose when the desired hose length $\hat{l}$ is defined to be equal to the hose length l, i.e., $l = \hat{l}$. Second, when the hose is overslack, as presented in Fig. 11(b), the hose length should be larger than its desired value, i.e., $l > \hat{l}$. Consequently, the hose slack degree μ_{slack} can be defined as

$$\mu_{\text{slack}} \triangleq \left| \frac{l - \hat{l}}{\hat{l}} \right| \tag{7}$$

which can be used to describe the hose state and predict the degree of the HWP. The slack degree $\mu_{\text{slack}} = 0$ indicates that the hose is in the desired state with no overslack. The more the slack degree μ_{slack} increases, the more the hose is bent, which indicates that a more serious HWP is ready to happen.

In order to obtain μ_{slack}, the method to obtain the desired hose length $\hat{l}$ should be given first. As shown in Fig. 11(a), the desired hose shape is a smooth curve, whose length $\hat{l}$ can be written as a function that depends on the drogue position $\boldsymbol{p}_d$ as

$$\hat{l} = f_{\hat{l}}\left(\boldsymbol{p}_d\right) \tag{8}$$

where $f_{\hat{l}}(\cdot)$ can be obtained by hose modeling methods [5], [8] or lookup table methods. However, in practice, precise expressions of $\hat{l}$ for different flight conditions (altitude and speed) are very complicated and unobtainable. Alternatively, an approximate estimation method for $\hat{l}$ is developed in this article. Based on the simulation results with the hose model [5], [8], the estimation expression for the desired length $\hat{l}$ approximates to a function of the straight-line distance of the drogue $\|\boldsymbol{p}_d\|$ as

$$\hat{l} \approx f'_{\hat{l}}\left(\|\boldsymbol{p}_d\|\right) \approx \frac{\|\boldsymbol{p}_d\|}{\|\boldsymbol{p}_{d0}\|} \cdot l_0 \tag{9}$$

where $\boldsymbol{p}_{d0}$ and l_0 are the initial equilibrium drogue position and hose length, respectively. The maximum estimated error $\varepsilon_{\hat{l}}$ for (9) is given by

$$\varepsilon_{\hat{l}} = \max_{\boldsymbol{p}_d \in \Omega} \frac{\left| \hat{l} - \frac{\|\boldsymbol{p}_d\|}{\|\boldsymbol{p}_{d0}\|} \cdot l_0 \right|}{\hat{l}} \tag{10}$$

where Ω denotes a safe region for the normal drogue movement. According to the simulation results, $\varepsilon_{\hat{l}}$ is very small, but still the following anti-HWP control method will well consider this error and hand it for robustness requirements.

3) *HWP Detection:* Safety is always the most fundamental requirement for any aerial refueling system. To avoid the damage of the HWP after an excessive or abnormal impact on the drogue, this subsection presents a method to detect the hose state and classify it into three situations based on its hazardous degree.

a) *Normal situation:* Ideally, the normal situation should be $\mu_{\text{slack}} = 0$; namely, the hose coincides exactly with the desired hose curve, as shown in Fig. 11(a). However, it is

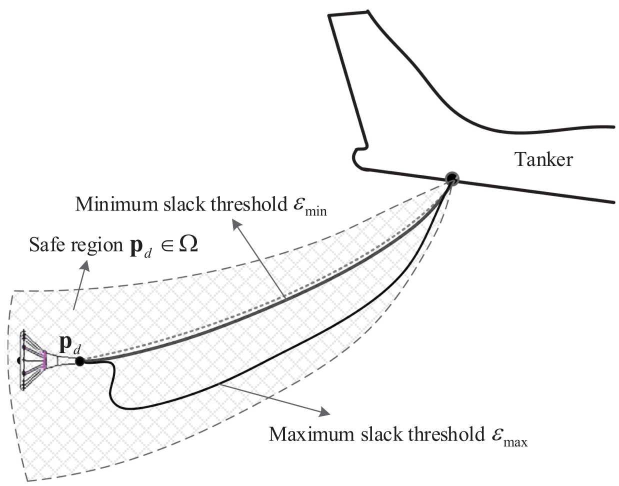

Fig. 12. Safety criteria for the hose–drogue system.

unreachable in practice due to the estimated error of (9) and other uncertain errors, such as the small fluctuation of the hose under atmospheric turbulence. Therefore, a minimum slack threshold $\varepsilon_{\min}$ is defined, as shown in Fig. 12. The normal situation of the hose is defined by the criterion

$$\mu_{\text{slack}} \leq \varepsilon_{\min} \text{ and } \mathbf{p}_d \in \Omega \tag{11}$$

where the threshold $\varepsilon_{\min}$ should cover the estimation error ($\varepsilon_{\min} > \varepsilon_{\hat{l}}$) and other uncertain errors for robustness requirements. For simplicity, consider $\varepsilon_{\min} = 2\varepsilon_{\hat{l}}$ for a 100% safe margin. In (11), the safe region $\mathbf{p}_d \in \Omega$ is presented as the meshed region in Fig. 12. If the drogue is out of this region ($\mathbf{p}_d \notin \Omega$), it indicates that an abnormal big swing is already appearing, and emergency measures should be taken immediately.

b) *Overslack situation:* The overslack situation is defined as that the hose slack degree μ_{slack} is out of "normal range" in (11), and it is within the controllable region for the HDU controller to safely reduce the slack degree μ_{slack} to the normal situation. Similar to (11), the overslack situation can be defined by the following criterion:

$$\varepsilon_{\min} < \mu_{\text{slack}} \leq \varepsilon_{\max} \text{ and } \mathbf{p}_d \in \Omega \tag{12}$$

where $\varepsilon_{\max}$ is the maximum slack threshold, as shown in Fig. 12, which is selected based on the safety requirement and controller performance.

c) *Unsafe situation:* The unsafe situation is defined as the complementary set of (11), (12)

$$\mu_{\text{slack}} > \varepsilon_{\max} \text{ or } \mathbf{p}_d \notin \Omega. \tag{13}$$

When the drogue–drogue system reaches this situation, it means that a serious HWP is happening or ready to happen. To ensure the safety of the hose-and-drogue system, emergency measures should be applied immediately, for example, rolling up the hose with the maximum speed to avoid a collision on the receiver aircraft.

For the aforementioned three situations, different control strategies will be adopted to avoid the HWP and ensure the safety of the drogue–hose system. When the hose is in the normal situation, it indicates that no impact or abnormal oscillation is happening on the drogue, so the traditional HDU control methods, as presented in Section IV, can be applied to reduce the drogue position fluctuation for improving the docking success rate. When the hose is in the unsafe situation, emergency control measures should be carried out to avoid further damage on the receiver aircraft or equipment. For example, the HDU controller rolls up the hose with the maximum speed to leave a safe distance between the hose and the receiver aircraft. Since the overslack situation is the most important stage to handle the impact on the drogue and avoid the HWP, the next subsection will focus on the anti-HWP controller design in this situation.

B. Anti-HWP Control

The objective of the anti-HWP controller for the HDU is to smoothly control the hose length to change the hose state from the overslack situation ($\varepsilon_{\min} < \mu_{\text{slack}} \leq \varepsilon_{\max}$) to the normal situation ($\mu_{\text{slack}} \leq \varepsilon_{\min}$). Then, the traditional HDU controller is capable of stabilizing the hose-and-drogue system to an equilibrium state in the normal situation.

First of all, a speed feed back control is given by

$$T_{\text{reel}} = T_{\text{hose}} - m_{\text{reel}} \cdot k_d \cdot \left(\dot{l} - \hat{\dot{l}}\right) \tag{14}$$

where $\hat{\dot{l}}$ is an indirect control input signal that indicates the desired increasing speed of the hose length, and $k_d > 0$ is a controller parameter. Substituting (14) into the HDU model (4) gives

$$\ddot{l} = \frac{T_{\text{reel}} - T_{\text{hose}}}{m_{\text{reel}}} = -k_d \cdot \left(\dot{l} - \hat{\dot{l}}\right) \tag{15}$$

which is an exponentially convergent system that ensures that the HDU tracks the given speed as $\dot{l} \to \hat{\dot{l}}$. Second, the desired speed input $\hat{\dot{l}}$ is further given by

$$\hat{\dot{l}} = -k_p \cdot \left(l - \hat{l}\right) \tag{16}$$

where $k_p > 0$ is a controller parameter. Note that, in practice, a saturation function can be added to (16) to prevent the drogue from pulling out the probe if the hose rolls up too fast. Finally, by combining (9), (14), and (16), the anti-HWP controller can be written as

$$\begin{aligned} T_{\text{reel}} = \; & T_{\text{hose}} + m_{\text{reel}} k_d k_p \frac{\|\mathbf{p}_d\|}{\|\mathbf{p}_{d0}\|} l_0 \\ & - m_{\text{reel}} k_d \cdot \dot{l} - m_{\text{reel}} k_d k_p \cdot l. \end{aligned} \tag{17}$$

The following theorem provides the convergence condition under which one can conclude the convergence property of the designed terminal iterative learning control (TILC) controller in (17).

THEOREM 1 Consider a hose-and-drogue system with the HDU structure described by (2) and (4). Suppose that 1) the hose state is in overslack situation (12) and 2) the anti-HWP controller is designed as (17) with its parameters satisfying

$$k_p > 0, \quad k_d > 0. \tag{18}$$

Then, the hose slack degree μ_{slack} can converge to zero, i.e., $\mu_{\text{slack}}(t) \to 0$.

PROOF Combining (15) and (16) gives

$$\ddot{l} + k_d \dot{l} + k_d k_p \left(l - \hat{l}\right) = 0. \tag{19}$$

By letting $\Delta l \triangleq l - \hat{l}$, for a constant value $\hat{l}$, (19) can be rewritten as

$$\Delta\ddot{l} + k_d \Delta\dot{l} + k_d k_p \Delta l = 0. \tag{20}$$

It can be observed from (20) that controller (17) is essentially a proportion differentiation controller with the proportion coefficient k_p and the differentiation coefficient k_d. Therefore, (20) is a stable second-order linear system when $k_d > 0$ and $k_d > 0$, which will converge exponentially to zero, i.e.,

$$\lim_{t\to\infty} \left|l(t) - \hat{l}\right| = \lim_{t\to\infty} |\Delta l(t)| = 0. \tag{21}$$

Then, according to the definition of μ_{slack} in (7), it can be derived from (21) that

$$\mu_{\text{slack}}(t) \triangleq \left|\frac{l(t) - \hat{l}}{\hat{l}}\right| = \frac{|\Delta l(t)|}{\hat{l}} \to 0 \tag{22}$$

which indicates that the hose slack degree μ_{slack} can converge to zero under controller (17).

According to Theorem 1, when the hose slack degree is in the range $\varepsilon_{\min} < \mu_{\text{slack}} \le \varepsilon_{\max}$, it will always converge to zero, which means the slack degree can eventually be reduced into region $\mu_{\text{slack}} \le \varepsilon_{\min}$. Then, the traditional HDU controller will take over the control privilege. According to [16], the hose-and-drogue system is a self-stabilizing system, and it will be stabilized to an equilibrium state under the effect of gravity, air drag, and air viscous.

C. Simulation Verification

A series of simulations are performed to verify the effect of the proposed anti-HWP controller. The basic parameters are listed in Table I, and additional parameters are given as follows:

$$\varepsilon_{\min} = 0.004,\ \varepsilon_{\max} = 0.05,\ k_d = 10,\ k_p = 3.$$

The variable-length hose–drogue model [8] with the link number $N = 20$ is used in these simulations for better simulation accuracy and display effect. A video has also been released to introduce the simulation environment and demonstrate the control effect of the proposed anti-HWP controller method. The URL of the video is https://youtu.be/s9XgGICqKtA.

Fig. 13 presents three typical comparative simulation results: 1) the simulation results (solid green curves in Fig. 13) with no HDU controller, where the HDU controller is not enabled, and the hose length remains unchanged during the whole simulation; 2) the simulation results (dotted red curves in Fig. 13) with the existing HDU control method, where the HDU controller is enabled to control the hose length to weaken HWP; and 3) the simulation results (dash blue curves in Fig. 13) with the proposed anti-HWP method,

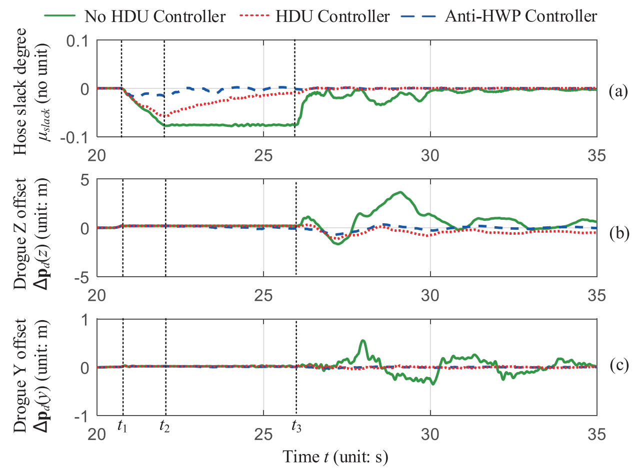

Fig. 13. Simulations of the probe-and-drogue system with and without an anti-HWP controller.

where the anti-HWP controller is enabled to control the hose length to avoid HWP safely. The above three simulations all contain the following stages.

1) The receiver flies close to the drogue from time 0 s to t_1.
2) The contact between the probe and the drogue happens at t_1.
3) The probe drives the drogue fly forward a distance from time t_1 to t_2.
4) The probe holds the drogue and remains relatively static from time t_2 to t_3.
5) The receiver suddenly breaks away from drogue at time t_3 and flies backward from time t_3 to 35 s.

The following can be observed from Fig. 13(a): 1) the hose slack degree increases to a large value for the simulation curve with no HDU controller, which indicates that a serious HWP is happening; 2) the hose slack degree increases to a medium value for the simulation curve with an HDU controller, but its slack degree is much smaller than the simulation curve with no HDU controller, which indicates that the existing HDU control methods can suppress the HWP but cannot completely avoid it; and 3) there is almost no hose slack for the simulation curve with the anti-HWP controller, which indicates that the HWP is successfully avoided. Fig. 14(a) and (b) shows the slack states of the hose with no HDU controller and with the proposed anti-HWP controller. Due to the overslack state of the hose, a significant HWP is observed in the simulation without the anti-HWP controller, which is reflected in the drastic position fluctuation along Y and Z directions in Fig. 13(b) and (c). By contrast, the hose and drogue states are both very steady with the proposed anti-HWP controller, and no HWP happens, as expected. The above results indicate that, compared with the existing HDU control methods, the proposed anti-HWP control method can effectively avoid the HWP and ensure the safety of hose-and-drogue systems.

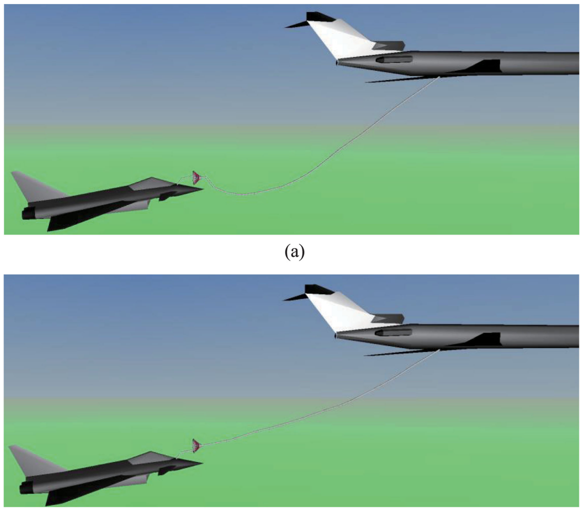

(a)

(b)

Fig. 14. Visual display of the hose-and-drogue systems under excessive contact. (a) Hose dynamics after excessive contact on the drogue. (b) Hose dynamics with the anti-HWP controller after excessive contact.

VI. CONCLUSION

Analysis of the dynamic of the drogue under the bow wave is critical when designing docking controllers and docking simulations. However, this problem is not considered comprehensively in the existing literature. This article integrates the HDU model, the bow wave model, and the variable-length hose–drogue model into an improved model. Then, two types of controllers are designed for HDU. One type is the commonly used controller used in the real PDR, and the other one is an improved one based on the commonly used controller. Based on the integrated model, the drogue dynamic models under different HDU controllers are obtained through system identification, and the performance of them is analyzed. By considering the effects of the HDU, the dynamics of the proposed method is in better agreement with the real experiment than our previous study. Meanwhile, the traditional HDU control methods mainly feed back the hose tension to reduce the drogue fluctuation and suppress the HWP to some extent, but it cannot avoid the HWP essentially. An anti-HWP control method is proposed to significantly reduce the effect of the HWP and improve the safety of aerial refueling systems. Finally, the effectiveness of the proposed modeling method and the anti-HWP control method is well verified by simulations and comparisons.

REFERENCES

[1] J.-S. Lee and K.-H. Yu
Optimal path planning of solar-powered UAV using gravitational potential energy
IEEE Trans. Aerosp. Electron. Syst., vol. 53, no. 3, pp. 1442–1451, Jun. 2017.

[2] J. L. G. Olavo *et al.*
Robust guidance strategy for target circulation by controlled UAV
IEEE Trans. Aerosp. Electron. Syst., vol. 54, no. 3, pp. 1415–1431, Jun. 2018.

[3] V. Roberge, M. Tarbouchi, and G. Labonté
Fast genetic algorithm path planner for fixed-wing military UAV using GPU
IEEE Trans. Aerosp. Electron. Syst., vol. 54, no. 5, pp. 2105–2117, Oct. 2018.

[4] P. R. Thomas, U. Bhandari, S. Bullock, T. S. Richardson, and J. L. Du Bois
Advances in air to air refuelling
Prog. Aerosp. Sci., vol. 71, pp. 14–35, 2014.

[5] K. Ro, T. Kuk, and J. W. Kamman
Dynamics and control of hose-drogue refueling systems during coupling
J. Guid., Control Dyn., vol. 34, no. 6, pp. 1694–1708, 2011.

[6] J. Vassberg, D. Yeh, A. Blair, and J. M. Evert
Numerical simulations of KC-10 wing-mount aerial refueling hose-drogue dynamics with a reel take-up system
In *Proc. 21st Appl. Aerodyn. Conf.*, 2003, Paper AIAA 2003-3508.

[7] J. Vassberg, D. Yeh, A. Blair, and J. Evert
Numerical simulations of KC-10 in-flight refueling hose-drogue dynamics with an approaching F/A-18D receiver aircraft
In *Proc. 23rd AIAA Appl. Aerodyn. Conf.*, 2005, Paper AIAA 2005-4605.

[8] H. Wang, X. Dong, J. Xue, and J. Liu
Dynamic modeling of a hose-drogue aerial refueling system and integral sliding mode backstepping control for the hose whipping phenomenon
Chin. J. Aeronaut., vol. 27, no. 4, pp. 930–946, 2014.

[9] K. Ro, H. Ahmad, and J. W. Kamman
Dynamic modeling and simulation of hose-paradrogue assembly for mid-air operations
In *Proc. AIAA Infotech@Aerosp. Conf.*, Seattle, WA, USA, 2009, Paper AIAA 2009-1849.

[10] Z. H. Zhu and S. A. Meguid
Elastodynamic analysis of aerial refueling hose using curved beam element
AIAA J., vol. 44, no. 6, p. 1317, 2006.

[11] K. Yue, L. Cheng, T. Zhang, J. Ji, and D. Yu
Numerical simulation of the aerodynamic influence of an aircraft on the hose-refueling system during aerial refueling operations
Aerosp. Sci. Technol., vol. 49, pp. 34–40, 2016.

[12] B. Chen, X. Dong, Y. Xu, and Q. Lin
Disturbance analysis and flight control law design for aerial refueling
In *Proc. Int. Conf. Mechatronics Autom.*, 2007, pp. 2997–3002.

[13] R. P. Dibley, M. J. Allen, and N. Nabaa
Autonomous airborne refueling demonstration phase I flight-test results
In *Proc. AIAA Atmos. Flight Mech. Conf. Exhib.*, Aug. 2007, Paper AIAA 2007-6639.

[14] Z.-B. Wei, X. Dai, Q. Quan, and K.-Y. Cai
Drogue dynamic model under bow wave in probe-and-drogue refueling
IEEE Trans. Aerosp. Electron. Syst., vol. 52, no. 4, pp. 1728–1742, Aug. 2016.

[15] X. Dai, Z.-B. Wei, and Q. Quan
Modeling and simulation of bow wave effect in probe and drogue aerial refueling
Chin. J. Aeronaut., vol. 29, no. 2, pp. 448–461, 2016.

[16] X. Dai, Q. Quan, J. Ren, Z. Xi, and K.-Y. Cai
Terminal iterative learning control for autonomous aerial refueling under aerodynamic disturbances
J. Guid., Control, Dyn., vol. 41, no. 7, pp. 1577–1584, 2018.

[17] X. Dai, Q. Quan, J. Ren, and K.-Y. Cai
Iterative learning control and initial value estimation for probe-drogue autonomous aerial refueling of UAVs
Aerosp. Sci. Technol., vol. 82, pp. 583–593, 2018.

[18] J. Ren, X. Dai, Q. Quan, Z.-B. Wei, and K.-Y. Cai
Reliable docking control scheme for probe-drogue refueling
J. Guid., Control, Dyn., vol. 42, no. 11, pp. 2511–2520, 2019.

[19] K. Ro and J. W. Kamman
Modeling and simulation of hose-paradrogue aerial refueling systems
J. Guid., Control, Dyn., vol. 33, no. 1, pp. 53–63, 2010.

[20] W. R. Williamson, E. Reed, G. J. Glenn, S. M. Stecko, J. Musgrave, and J. M. Takacs
Controllable drogue for automated aerial refueling
J. Aircr., vol. 47, no. 2, pp. 515–527, 2010.

[21] K. Ro, T. Kuk, and J. Kamman
Active control of aerial refueling hose-drogue systems
presented at the AIAA Guid., Navigat., Control Conf., 2010, Paper AIAA 2010-8400.

[22] U. Bhandari, P. R. Thomas, S. Bullock, T. S. Richardson, and J. du Bois
Bow wave effect in probe-and-drogue aerial refuelling
presented at the AIAA Guid., Navigat., Control Conf., 2013, Paper AIAA 2013-4695.

[23] L. Ljung
MATLAB: System Identification Toolbox: User's Guide Version 4. Natick, MA, USA: Mathworks, 1995.

[24] G. F. Franklin, J. D. Powell, A. Emami-Naeini, and J. D. Powell
Feedback Control of Dynamic Systems, vol. 3, 6th ed. London, U.K.: Pearson Education, 2009.

[25] M. D. Tandale, R. Bowers, and J. Valasek
Trajectory tracking controller for vision-based probe and drogue autonomous aerial refueling
J. Guid., Control, Dyn., vol. 29, no. 4, pp. 846–857, 2008.

Xunhua Dai received the B.S. and M.S. degrees in 2013, and 2016, respectively, in automation science and electrical engineering from Beihang University, Beijing, China, where he is currently working toward the Ph.D. degree in navigation, guidance and control with the School of Automation Science and Electrical Engineering.

His main research interests include reliable flight control, learning control, model-based design, and optimization of unmanned aerial vehicles.

Zi-Bo Wei received the Ph.D. degree in automation science and electrical engineering from Beihang University, Beijing, China, in 2016.

He is currently an Engineer with the Shanghai Aircraft Design and Research Institute, Shanghai, China. His main research interests include automatic flight system design, automatic flight control law design, and aerial refueling.

Quan Quan received the B.S. and Ph.D. degrees in automation science and electrical engineering from Beihang University, Beijing, China, in 2004, and 2010, respectively.

Since 2013, he has been an Associate Professor with Beihang University, where he is currently with the School of Automation Science and Electrical Engineering. His research interests include reliable flight control, vision-based navigation, repetitive learning control, and time-delay systems.

Kai-Yuan Cai received the B.S., M.S., and Ph.D. degrees in automation science and electrical engineering from Beihang University, Beijing, China, in 1984, 1987, and 1991, respectively.

He has been a Full Professor with Beihang University since 1995. He is a Cheung Kong Scholar (Chair Professor), jointly appointed by the Ministry of Education of China and the Li Ka Shing Foundation of Hong Kong in 1999. His main research interests include software testing, software reliability, reliable flight control, and software cybernetics.